

# Varicella Zoster Virus ORF25 Gene Product: An Essential Hub Protein Linking Encapsidation Proteins and the Nuclear Egress Complex



Published in final edited form as:
*J Proteome Res*. 2011 December 2; 10(12): 5374–5382. doi:10.1021/pr200628s.

# Varicella Zoster Virus ORF25 gene product: an essential hub protein linking encapsidation proteins and the nuclear egress complex

**Maria G. Vizoso Pinto**[1,*], **Venkata R. Pothineni**[1], **Rudolf Haase**[1], **Mathias Woidy**[2], **Amelie S. Lotz-Havla**[2], **Søren W. Gersting**[2], **Ania C. Muntau**[2], **Jürgen Haas**[1,3], **Marvin Sommer**[4], **Ann M. Arvin**[4], and **Armin Baiker**[1,5]

[1]Max von Pettenkofer-Institute, Ludwig-Maximilians-University, Munich, Germany

[2]Department of Molecular Pediatrics, Dr. von Hauner Children's Hospital, Ludwig-Maximilians-University, Munich, Germany

[3]Division of Pathway Medicine, University of Edinburgh, U.K.

[4]Stanford University, Department of Pediatrics, Stanford, USA

[5]Bavarian Health and Food Safety Authority, Oberschleissheim, Germany

## Abstract

Varicella zoster virus (VZV) ORF25 is a 156 amino acid protein belonging to the approximately 40 core proteins that are conserved throughout the *Herpesviridae*. By analogy to its functional orthologue UL33 in Herpes simplex virus 1 (HSV-1), ORF25 is thought to be a component of the terminase complex. To investigate how cleavage and encapsidation of viral DNA links to the nuclear egress of mature capsids in VZV, we tested ten VZV proteins that are predicted to be involved in either of the two processes for protein interactions against each other using three independent protein-protein interaction (PPI) detection systems: the yeast-two-hybrid (Y2H) system, a luminescence based MBP pull-down interaction screening assay (LuMPIS) and a bioluminescence resonance energy transfer (BRET) assay. A set of 20 interactions was consistently detected by >2 methods and resulted in a dense interaction network between proteins associated in encapsidation and nuclear egress. The results indicate that the terminase complex in VZV consists of ORF25, ORF30 and ORF45/42, and support a model in which both processes are closely linked to each other. Consistent with its role as a central hub for protein interactions, ORF25 is shown to be essential for VZV replication.

### Keywords

varicella zoster virus; ORF25; encapsidation; nuclear egress complex; LuMPIS; BRET; Y2H; terminase

## INTRODUCTION

Varicella-zoster virus (VZV) causes chickenpox upon primary infection and establishes latency in the dorsal root ganglia, from where it may reactivate causing herpes zoster. As a member of the α-Herpesviruses VZV belongs to the most complex viruses known. The

[*]**Corresponding author**: Mailing Address: Max von Pettenkofer-Institute, Department of Virology, Pettenkoferstr. 9a, 80336, Munich, Germany. Phone: +49-(0)89-5160-5231, Fax: +49-(0)89-5160-5292, vizoso@mvp.uni-muenchen.de; guadalupevizoso@yahoo.com.

virion particles consist of a double-stranded (ds) DNA genome packaged into a nucleocapsid, a proteinaceous matrix called the tegument, and a cell-derived lipid envelope [1]. The dsDNA replication of α-herpesviruses is believed to follow a rolling-circle mechanism, where concatemers of genomes arranged in a head-to-tail fashion are formed. The cleavage of single genomes is tightly coupled to their energy-dependent packaging into precapsids, a process mediated by multi-protein complexes, which resembles the packaging of genomes in the tailed dsDNA bacteriophages [1, 2]. In HSV-1, at least seven proteins are known to be responsible for these processes: UL6, UL15, UL17, UL25, UL28, UL32 and UL33 [3, 4]. Three of them, HSV-1 UL15, UL28 and UL33 have been shown to interact with each other and are considered to form the terminase complex [5, 6]. Deletion of these genes is lethal as the viruses are not able to package the dsDNA into the capsid [4, 7, 8].

VZV ORF25, the orthologue of HSV-1 UL33, is a 156 aa protein which belongs to a set of approximately 40 core proteins that are conserved throughout the *Herpesviridae*. In HSV-1, UL33 has been shown to be essential and involved in DNA packaging [3, 4, 9]. Within a comprehensive Y2H analysis of the VZV protein interaction network, we previously showed that VZV ORF25 constitutes a central hub interacting with many other VZV proteins [10]. Interestingly, VZV ORF25 interacts with only four cellular proteins (unpublished results). Recently, Visalli et al. have shown that ORF25 interacts with two components, i.e. ORF30 and ORF45/42 (HSV-1 UL28 and UL15), of the putative terminase complex by pull-down assays in an *in vitro* translation system [11]. Not yet well understood, however, is the linkage between cleavage/encapsidation of viral DNA and the nuclear egress of mature capsids.Here we investigate the interactions of all the VZV proteins that are predicted to be related to the encapsidation process and the nuclear egress complex (NEC) by means of three independent protein-protein interaction (PPI) detection systems: Y2H, luminescence based MBP pull-down interaction screening (LuMPIS) and bioluminescence resonance energy transfer (BRET) [10, 12]. Furthermore, we demonstrate that ORF25 is essential for virus replication by generating ORF25 mutant viruses using a cosmid based system.

## MATERIALS AND METHODS

### Recombinatorial Cloning of VZV ORFs

The nucleotide sequences of all VZV ORFs used in this study were obtained from the ncbi (http://www.ncbi.nlm.nih.gov/). BP recombination reactions of VZV ORFs into pDONR207 (Invitrogen, Germany) were performed as described earlier [10, 13]. LR recombination reactions using LR-clonase II enzyme mix (Invitrogen, Germany) were performed according to the manufacturers' instructions. Briefly, pENTR207-VZV-ORF vectors containing VZV-ORFs flanked by *attL*-sites were recombinatorially cloned into the *attR*-sites of the customized vectors pCR3-MBP-N-[rfB], pCR3-eGFPLuc-N-[rfB] [12], pCR3-Venus-N-[rfB] and respective BRET destination vectors with N- or C-terminal coding sequence of *Renilla* luciferase (Rluc) or yellow fluorescence protein (YFP). The vector pCR3-Venus-N-[rfB] has been constructed by insertion of a customized cassette consisting of 5′-*Hind*III-ATG-[Venus]-*EcoR*V-[ccdB/CmR(rfB)]-*EcoRV*-3′ into the backbone of the pCR3 (Invitrogen, Germany). LR clonase reactions were incubated at 37°C for 2 h and subsequently transformed into chemically competent *E. coli* DH5α. Plasmid DNA of individual colonies grown on LB-plates supplemented with 100 μg/ml ampicillin (Sigma-Aldrich, Germany) was isolated and the integrity of the resulting pCR3- based vectors was verified by restriction analysis.

### Construction of VZV cosmids and generation of ORF25 mutant viruses

The complete genome of the parental OKA (pOKA) VZV strain has been subcloned as four overlapping fragments within the cosmids: pvSpe14, pvFsp73, pvSpe23ΔAvrII, and

pvPme2 [14, 15]. For easier handling, the pvSpe14 cosmid was split into two smaller cosmids designated pNhe and pPvu within this work (Fig. 1, lane 3)**.** For the construction of pNhe, the original vector pvSpe14 was digested with *NheI*, treated with Klenow enzyme and subsequently digested with *AscI*. The 26964bp *AscI* / (*NheI*-)blunt end fragment comprising the VZV- specific nucleotides 1 (*AscI*) - 26964 (*NheI*) of pvSpe14 was isolated and inserted into SuperCos vector (Stratagene, USA). For this purpose, SuperCos vector was digested with *AvrII*, blunt ended with Klenow enzyme and digested with *AscI*. The religation of blunt ended *NheI* and *AvrII* sites reconstituted a functional *NheI* site. Prior to cosmid transfections, the SuperCos vector part of pNhe was separated from the 26964bp genomic VZV-sequence by *AscI* and *NheI* double digest. For the construction of pPvu, the original vector pvSpe14 was digested with *PvuI*. The 21602bp *PvuI* fragment comprising the VZV-specific nucleotides 24687 - 40080 of pvSpe14 and approximately 5000bp of its 6800bp SuperCos vector backbone was isolated and ligated to an 1800bp, *PvuI*-digested PCR-fragment designed to reconstitute the functional (full length) SuperCos vector backbone within pPvu. The latter PCR-fragment was amplified from pvSpe14, by using the primers “45215upper” (5′- TTCCGACCCTGCCGCTTACC-3′) and “end+PvuI lower” (5′-TCACCGATCGGGCGCGCCGGATCCTTTAGT-3′). Prior to cosmid transfections, the SuperCos vector part of pPvu was separated from the 15393bp genomic VZV-sequence by *AscI* digest.

The strategy for the deletion of endogenous ORF25 was critical, since its reading frame overlapped with the reading frame of ORF26 (Fig. 1, lane 4). Therefore, deletion of ORF25 was achieved by introducing the stop codon TAA at amino acid position 2, leading to a silent mutation within ORF26. For the introduction of the respective mutation, the 4.2kb *ApaI* / *NheI* fragment of pNhe was subcloned into the multiple cloning site of pGFP-C1 (Clontech, USA), resulting in the shuttle vector pGFP[4.2kb]. PCR mutagenesis was performed by two rounds of PCR within the 800bp *ApaI* / *NotI* fragment of pGFP[4.2kb]. The resulting *ApaI* / *NotI* PCR fragment comprising the ORF25 deletion and its endogenous promoter was TA-cloned into pGEM-T easy, verified by sequencing, placed back into pGFP[4.2kb] and finally into the pNhe cosmid backbone resulting in the cosmid pNheΔORF25 (Fig. 1, lane 4).

For the generation of pOKA-ORF25 (rescue) mutant viruses within the pOKAΔORF25 backbone, wild type ORF25 mutant and its endogenous promoter cassette was isolated as an *AvrII* fragment from its respective pGEM-T easy construct and integrated into the single *AvrII* site of pvSpe23ΔAvrII [15] (Fig. 1, lane 5). The cosmid pvSpe23-@ORF25-WT, containing the wildtype ORF25 sequence was constructed analogously as control. The integrity ofthe generated pvSpe23ΔAvrII-based (rescue) cosmids was verified by restriction analysis and deep sequencing (LGC Genomics, Germany).

## Cosmid transfections

The pvSpe23ΔAvrII-based cosmids and the other four VZV cosmids pvFsp73, pvPme2, pPvu, and pNheΔORF25 (or pNhe), were electroporated into Top 10F’ competent cells (Invitrogen, Germany), grown in LB containing kanamycin and ampicillin, and purified with a NucleoBond plasmid maxi prep kit (Macherey-Nagel GmbH, Germany). Cosmids were digested with *AscI* (*AscI* and *NheI* in case of pNhe or pNheΔORF25), heat inactivated for 10 min at 65°C and mixed in water to a final concentration of 100 ng/μl of pvFsp73, pvPme2, pPvu, and pNheΔORF25 (or pNhe), and 50 ng/μl of pvSpe23ΔAvrII-based cosmid. Typical calcium phosphate transfections were done in human MeWo cells utilizing the CalPhos™ Kit (Clontech, USA) according to the manufacturers’ instructions. After transfection, MeWo cells were passed at a 1:3 ratio every 3 to 4 days until plaques were visible. The reconstituted recombinant viruses were named: pOKA (derived from pvFsp73, pvPme2, pNhe, pPvu, pvSpe23ΔAvrII) and pOKAΔORF25-R- WT (derived from pvFsp73, pvPme2,

pNheΔORF25, pPvu, pvSpe23-@ORF25-WT. The integrity of all reconstituted viruses was verified by sequencing (LGC Genomics, Germany).

## Antiserum preparation

For the generation of a polyclonal antiserum against VZV ORF25, *E. coli* BL21 (Invitrogen, Germany) were transformed with pETG-His-N-ORF25 [13]. His-tagged ORF25 was purified by Ni-NTA affinity chromatography (Qiagen, Germany) and used for the immunization of rabbits in our *in house* animal facility (Max von Pettenkofer Institute). Preimmune sera and sera derived from different bleedings were analyzed by western blot and immunfluorescence (data not shown).

## Cell lines

MeWo (ATCC HTB-65) cells used for propagation of recombinant wild type and mutant parental pOKA strains were grown in MEM (Invitrogen, Germany), supplemented with 10% FCS (PAA, Germany), 1% non essential amino acids (Invitrogen, Germany), 100 units/ml pencillin, 0.1 mg/ml streptomycin and fungizone (Invitrogen, Germany). Hela cells were grown in D-MEM (Invitrogen, Germany) supplemented as described above. HEK 293 T (ATCC CRL-11268) cells were grown in the same medium as Hela (ATCC CCL-2) but additionally supplemented with 20 μg/ml G418 (PAA Laboratories, USA). COS7 (DSMZ ACC 60) cells were cultured in hyperflask cell culture vessels (Corning, Germany) in RPMI 1640 with stable glutamin (4.5 g/l) (PAA, Germany) supplemented with 10 % FCS (PAA, Germany), 100 units/ml penicillin, 0.1 mg/ml streptomycin and 0.25 μg/ml mphotecerin B (PAA, Germany).

## Immunofluorescence microscopy

To examine transfected cells by immunofluorescence microscopy, Hela cells were grown on glass slides placed on to 12-well cell culture plates and transiently transfected with pCR3-N-Venus-ORF25 with FugeneHD™ transfection reagent. After 48 h, the cells were fixed in ice-cold 4% paraformaldehyde for 10 min at 4°C, DAPI stained and washed three times with phosphate-buffer-saline (PBS). To evaluate if a second protein influenced ORF25 transient localization, co-transfection experiments were done using pCR3-N-MBP-ORFx (x= ORF24, ORF25, ORF26, ORF27, ORF30, ORF34, ORF45/42, ORF43, ORF46, ORF54, ORF62 and ORF63 (IE63)) or pCR3-N-ORF63. After blocking, cells were incubated with monoclonal anti-MBP (New England Biolabs, Germany) (1:10,000) at room temperature (RT) for 3 h on a shaking device. Cells were washed three times with PBS at room temperature and were incubated for 1 h with the secondary antibody (goat anti-mouse-A563, Invitrogen). Cells were washed with PBS and slides were mounted with Vectashield (Vector Laboratories, USA).

To examine infected cells by immunofluorescence microscopy, MeWo cells were grown in cell culture slides and infected with recombinant pOKA viruses. Four days post-infection, cells were fixed in 4% ice-cold paraformaldehyde for 10 min at 4°C. After fixation, a double IF staining was carried as described above using a polyclonal ORF25 rabbit antiserum (1:500) and a mouse monoclonal anti-IE63 (1:500) as primary antibodies and goat anti-rabbit-A488 and anti-mouse-A563 as secondary antibodies. (1:400, Invitrogen).

For time course IF experiments, infected inoculum cells were differentiated from uninfected cells by labelling with orange CellTracker (CMRA; Invitrogen). The orange cell tracker is retained within the labelled cells and is not released into the medium. The uninfected Mewo cells were seeded on the glass cover slips and were grown to 90% confluency. The uninfected cells were infected with CMRA labelled inoculum cells with a virus titre of $4 \times 10^3$ PFU. Inoculum cells were allowed to settle and were grown at 37°C. Cells were fixed

with 2% formaldehyde at 2, 4, 6, 9 and 12 h. Two cover slips were examined at each time point in all experiments, and two independent time course experiments were performed to evaluate the kinetics of expression of each VZV protein. After fixation, IF staining was carried as described above.

### Luciferase-based detection MBP-pull down interaction screen (LuMPIS)

LuMPIS was performed as described before [12]. Briefly, semiconfluent HEK 293 T cells grown in 12-well plates were transfected with the respective prey and bait vectors using FuGENE HD™ as transfection reagent. Transfected HEK 293 T cells were grown for 48 h and then lysed in 500 µl lysis buffer (20 mM Tris-HCl, 200 mM NaCl, 1 mM EDTA, 0.05 % Tween 20™, 5 µg/ml Leupeptin, 5 µg/ml DNAse I, 2.5 mg/ml BSA, pH 7.5) by sonication (5 pulses of 15 seconds) at 4°C. Lysates were cleared by centrifugation at 13,000 *g* at 4°C for 10 min and then diluted 1:10 in washing buffer (20 mM Tris-HCl, 200 mM NaCl, 1 mM EDTA). MBP tagged bait proteins were captured by using 100 µl of pre-equilibrated 50 % amylose beads slurry (New England Biolabs, Germany). After washing the amylose beads four times with 200 µl washing buffer, the captured MBP tagged bait proteins were eluted with 150 µl 10 mM maltose using a vacuum Manifold (Millipore, Germany). The co-eluted eGFP-Luc tagged prey proteins were detected by measuring luciferase activity in 50 µl eluate after addition of 50 µl luciferase assay reagent (Promega, Germany) using an Optima FLUOstar Luminometer system (BMG LABTech, Germany). The Luminescence Intensity Ratio (LIR) was calculated as LIR = ($Eluate_{\text{eGPF-Luc tagged prey \& MBP tagged bait}}$: $Lysate_{\text{eGFPLuc tagged prey \& MBP tagged bait}}$) / ($Eluate_{\text{negative control}}$: $Lysate_{\text{Negative control}}$). The negative control (i.e. eGFP-Luc tagged prey expression vector co-transfected with the empty MBP vector) was performed for each prey protein. Two independent experiments (in quaduruplicate) were done. The expression of N- eGFPLuc-tagged ORFs was tested by inverse fluorescence microscopy before starting the cell lysis and afterwards by measuring the luciferase activity of the lysates. In previous experiments, we have also checked by westernblot that the corresponding N-MBP-tagged VZV ORFs were appropriately expressed under the same experimental conditions. The data were statistically analysed by ANOVA ($P<0.05$) followed by Dunnett's post hoc test.

### Bioluminescence resonance energy transfer (BRET)

BRET analysis was performed as described before [12]. Briefly, binary interactions were tested in all eight possible combinations of the proteins of interest either fused to Rluc or YFP. All combinations were tested in duplicates and 2 independent experiments. For each interaction, COS7 cells were co-transfected with a total of 1 µg DNA at acceptor to donor ratios of 3:1 and incubated at 37°C. Luciferase signals were acquainted after 24 h upon addition of coelenterazine (30 µM) as the Rluc substrate to the living cells. Light emission was collected over 10 s at 475 nm (Rluc-signal) and 535 nm (BRET-signal). The BRET-ratio was calculated using (($BRET_{probe} - Rluc_{probe} * cf$) / $Rluc_{probe}$), where $cf = BRET_{control} / Rluc_{control}$ is a correction factor obtained from cells expressing Rluc fusion protein alone. Luminescence signals detected at 485 nm served as a control showing that the proteins of interest tagged to Rluc (energy donor) are efficiently expressed. The BRET ratio was only calculated for luminescence signals at 485 nm exceeding a background threshold level (interval of the mean value and the ninefold standard error of a non-transfected control). Sufficient expression of YFP tagged proteins was validated by fluorescence microscopy following BRET measurement.

# RESULTS

## Effect of ORF25 deletion on viral replication

First, we tested whether we could generate a ORF25 knock-out VZV virus mutant using an established cosmid system[14] modified in this work, however no infectious virus was reconstituted from eight independent transfection experiments when ORF25 was deleted. In all cases, infectious VZV was recovered when intact (wild type) ORF25 was inserted into pvSpe23 AvrII, in the context of the genomic deletion of ORF25, or when the wildtype set of cosmids was used, indicating that ORF25 is an essential protein for VZV replication. Furthermore, the reconstituted revertant showed no differences in replication as compared to the wild type, suggesting that the observed lethal phenotype of the knock-out mutant was due to the essential character of ORF25 and not to secondary mutations (data not shown). In addition, the ORF25 mutation did not revert to wild type as confirmed by PCR and sequencing.

## Intracellular localization of ORF25

Coverslips were seeded with MeWo cells and infected with pOKA to study the localization of ORF25 during VZV replication using a polyclonal rabbit anti-ORF25 antibody. In the context of viral infection at 48 h, ORF25 localized to the nucleus, forming globular domains occupying large parts of it, which resembled the typical arrangement of replication compartments and correlates with the localization of IE63 at early stages of infection (Fig. 2A, upper panel). In adition, ORF25 also localized diffusely to the cytoplasm. ORF25 individually expressed by transient transfection into Hela cells was localized to both the nucleus and the cytoplasm, but rather than forming globular structures in the nucleus it presented a diffuse localization (Fig. 2A, lower panel). When co-transfecting ORF25 with N-MBP tagged ORFs as indicated in the methods section and in case of IE63 also with the untagged form, no changes were observed in the transient ORF25 distribution in Hela cells (data not shown).

## ORF25 expression kinetics after infection

To investigate the kinetics of expression of ORF25, a differential labelling protocol was used to distinguish newly infected cells from infected inoculum cells. In addition, we also studied two well known immediate early (IE) and early proteins (E), namely IE63 and ORF47, respectively at intervals of 4, 6, 9 and 12 h after infection (Fig. 2B). Using a regular fluorescence microscope, the expression of both IE63 and ORF47 could be detected as early as 4 h post infection. Both proteins showed the typical staining already described for these proteins in the literature, with IE63 localized mainly to the nucleus and ORF47 cytoplasmatic. In contrast, ORF25 was not detected until 9 h post infection, indicating that this protein is expressed at later stages in infection. Similarly to IE63, ORF25 also showed nuclear staining characterized by globular domains (Fig. 2B). In addition, ORF25 could also be clearly detected in the cytoplasm, whereas IE63 showed very weak cytoplasmatic staining at this stage.

## ORF25 self-interaction

In order to study which domains of ORF25 are responsible for self-interaction, full length ORF25 and its N-terminal (aa 1 - 80) and C-terminal (aa 81 - 156) domains were subjected to Y2H and LuMPIS analysis. In both assays we found that the C-terminus of ORF25 is mainly involved in the self-interaction (Fig. 3).

### Analysis of PPI between ORF25 and VZV components of the terminase complex, NEC and proteins involved in DNA packaging

The PPI between ORF25 and ten proteins whose orthologues in other α-herpesviruses have been related to the encapsidation and nuclear egress process - i.e. ORF24 (UL34), ORF25 (UL33), ORF26 (UL32), ORF27 (UL31), ORF30 (UL28), ORF34 (UL25), ORF45/42 (UL15), ORF43 (UL17), ORF46 (UL14) and ORF54 (UL6) - were selected and investigated by three independent PPI testing systems: Y2H, LuMPIS and BRET. ORF25 interacted with seven of the proteins tested and itself in the Y2H screen [10, 16], with eight and itself in LuMPIS and with all of them apart from ORF24 in BRET (Table 1). As a result, ORF25 interacts with itself and seven other proteins with a high fidelity score, which suggests that ORF25 plays a central role in the encapsidation and nuclear egress process.

### Comprehensive analysis of PPI between VZV components of the terminase complex, NEC and other proteins involved in DNA packaging

For a more comprehensive analysis of PPI related to encapsidation and nuclear egress process, ORF25 and the ten relevant VZV proteins were analyzed systematically by Y2H, LuMPIS and BRET. VZV protein interaction screens based on Y2H analyses were recently published by members of our group [10, 16]. In the work of Stellberger et al., VZV ORFs were cloned as N- and C-terminal fusion proteins to the Gal4DNA binding (bait) and Gal4 activation (prey) domains and tested against each other in four combinations (NN, NC, CC, CN) using a matrix approach [10, 16]. Fig. 4A summarizes the results of the 400 tested protein-protein configurations [45 possible binary interactions × 4 possible $\text{combinations}_{(\text{NN, NC, CC, CN})}$ × 2 $\text{directions}_{(\text{as prey or bait})}$ + 10 possible self interactions × 3 possible $\text{combinations}_{(\text{NN, NC, CC, CN})}$ × 1 direction] among 10 ORFs analyzed within the comprehensive Y2H screen [10, 16]. In this approach, an interaction was considered positive if at least one of the combinations was positive (depicted as a full box in the matrix chart, Fig. 4A). The Y2H analysis revealed 23 binary interactions between the ten proteins that were tested (Fig. 4A).

The LuMPIS method is highly sensitive and can detect PPI with binding affinities of at least 10 μM[12]. In this assay, the ten VZV proteins were assayed as N-terminal fusion proteins (NN). Fig. 4B summarizes the results of the 100 tested protein-protein configurations [45 possible binary interactions x 1 possible $\text{combination}_{(\text{NN})}$ x 2 $\text{directions}_{(\text{as prey or as bait})}$ + 10 possible self interactions x 1 possible $\text{combinations}_{(\text{NN})}$] detected by LuMPIS. The analysis of the data generated by LuMPIS revealed 30 binary interactions between the 10 tested proteins. Seven PPI, which were found by the permutated Y2H screen, namely ORF24-ORF25, ORF24-ORF26, ORF24-ORF34, ORF24-ORF46, ORF30-ORF45/42, ORF34-ORF43 and ORF45/42-ORF45/42 were not detected by LuMPIS nor BRET (Fig. 4). On the other hand, fourteen PPI, which were not found in the Y2H screen, were detected by LuMPIS. These interactions were ORF25-ORF54, ORF26-ORF30, ORF26-ORF34, ORF26-ORF46, ORF26-ORF54, ORF27-ORF34, ORF27-ORF45/42, ORF30-ORF30, ORF34-ORF27, ORF34-ORF34, ORF34-ORF54, ORF43-ORF43, ORF43-ORF54 and ORF54-ORF54 (Fig. 4B).

In order to validate the PPI in real time in living cells, BRET was performed as described earlier [12]. For this purpose, the ten selected VZV proteins were N- and C- terminally fused to Rluc (donor) or YFP (acceptor), respectively, and tested against each other in all possible tag combinations. Fig. 4C summarizes the results of the 400 protein-protein configurations [45 possible binary interactions x 4 possible $\text{combinations}_{(\text{NN, NC, CC, CN})}$ × 2 $\text{directions}_{(\text{as donor or acceptor})}$ + 10 possible self interactions × 4 possible $\text{combinations}_{(\text{NN, NC, CN, CC})}$ × 1 direction] tested by BRET. We considered a PPI positive for BRET when at least one of the tested configurations was positive. Within this assay, 17

PPI could be detected. Three of these interactions were not found in either Y2H or LuMPIS (i.e. the ORF46 self-interaction, the ORF25-ORF46 and the ORF34-ORF46 interactions). Noticeably, only one of the ORF45/42 interactions, namely ORF45/42-ORF25 could be detected using this assay.

Using Y2H as the gold standard for PPI detection, we calculated the sensitivity and specificity of LuMPIS and BRET (Supplementary Table 1). While LuMPIS had a higher sensitivity (69.56% vs. 47.82%), BRET presented higher specificity (78.57% vs. 61.11%).

## DISCUSSION

Previous studies suggested that HSV-1 UL33 is an integral component of the terminase complex involved in the cleavage and packaging of HSV-1 DNA [4, 17]. In agreement with its postulated role in virus replication, UL33 has been shown to be essential [18]. Visalli et al. [11] hypothesized that VZV ORF25 is a component of the terminase complex and we show for the first time, that ORF25 is essential for VZV replication. The UL33 gene product is a highly conserved protein in α-herpesviruses, with the region comprising aa 101-130 being one of the most-well-conserved portions of the genome[4]. ORF25 interacts with itself via its C- terminal domain, which comprises this conserved tegion. The fact that the ORF25 full-length interaction was stronger than the PPI with the C-terminal domain may be due to differences in protein folding.

HSV-1 UL33 localizes mainly to the cytoplasm when transiently expressed, and to replication compartments in virus infected cells [4, 17]. A similar behaviour was observed for ORF25 but, in this case, a diffuse nuclear localization was also evident under transient conditions using Venus-tagged ORF25. Furthermore, we could not find a second viral protein that influenced ORF25 localization when transiently co-transfected (results not shown), in contrast to the effects of UL15 of HSV-1 [3] and UL14 of HSV-2 [17] on UL33. Wang et al. [19] have shown that proteins of up to about 110 kDa may diffuse through the nuclear pores. Thus, it is possible that ORF25, which is <20 kDa, may use this mechanism to translocate to the nucleus in the absence of an NLS.

In order to overcome the limitations due to the highly cell-associated nature of VZV, which makes it very difficult to obtain synchronous infections, we stained the inoculum cells to differentiate newly infected cells from inoculum using a similar approach as Reichelt et al. [20]. ORF25 was detected after IE63 and ORF47, which are considered IE and E proteins, respectively. Reichelt et al. [20] showed that VZV DNA replication was detectable at 4 hpi and virion assembly and envelopment by 9 hpi, which would correlate with the expression of ORF25 and its postulated involvement in packaging the viral DNA into preformed capsids.

LuMPIS, BRET and Y2H analysis revealed that ORF25 interacts with itself, and that the interaction domains comprise regions in the C-terminal domain. For studying the PPI of proteins involved or related to the encapsidation and nuclear egress process, we used three independent systems based on different principles and host cells as a strategy to reduce false positive and false negative rates. By doing so, we combined the advantages of each system, which reduced the possibility that an apparent interaction was a random occurrence (i.e. increased specificity) and also allowed the detection of interactions that might otherwise not have been identified (i.e increased sensitivity). The detection of protein interactions between membrane proteins is highly impaired or impossible using the Y2H system, since PPI that activate the auxotrophy are required to occur in the nucleus [21], and proteins artificiallly expressed in yeast may be misfolded or only partially folded. Nevertheless, Braun et al. [22] showed that Y2H is not prone to detect more false positives than other assays, and therefore

we used it as gold standard to calculate the sensitivities and specificities of the other two assays used here. LuMPIS showed a higher sensitivity than BRET (69.56% and 47.82%, respectively), i.a. a higher ability to identify positive results. Recently, five different types of assays detecting binary protein interactions were compared with a reference set of PPIs and the highest assay sensitivity was found for LUMIER [22], which has a similar principle as LuMPIS. Within the LuMPIS screen, we also found some novel interactions, which were not detected by the permutated Y2H screen (Fig. 4B). One of the main reasons could be that the transient PPI in LuMPIS is studied in the intracellular environmental context where the interaction usually takes place, it overcomes known expression problems of VZV ORFs due to their low GC content and also offers other advantages such as better solubilisation of the bait and high sensitivity of detection due to the luciferase [12].

BRET is a very powerful technique for the detection of PPI in living cells. The method overcomes the problem of false positive PPI caused by the artificial expression in the same cellular compartment, and is particularly useful for the detection of PPIs between membrane proteins. Bioluminescence resonance energy transfer only occurs if the acceptor-donor pair has a distance of <10 nm, a positive BRET-signal is therefore generally indicative of a physical interaction between proteins of interest. However, random collision of overexpressed protein pairs may result in unspecific energy transfer detected as “bystander” BRET signal [23, 24]. Due to the dipole-dipole nature of the resonance energy transfer mechanism, the relative orientation of the interaction partners may also affect the signal [21, 25]. Moreover, BRET tags may interfere with the interacting domains of the proteins of interest and thus impede physiological binding. To minimize these effects, we have tested all protein pairs in all possible configurations (Fig. 4C). BRET presented a lower number of false positives, which results in a higher specificity (78.57%) than LuMPIS (61.11%) (Supplementary Table 1). In total, only three interactions detected by BRET could not be confirmed by the other two assays.

The PPI chart (Fig. 5A) depicts graphically the binary PPI identified by using three independent systems: Y2H, LuMPIS and BRET. We considered the interactions that were found in all three assays to be high fidelity interactions (Fig. 5A), the PPI found in two assays as medium fidelity (Fig. 5A) and the ones found in only one of the systems as low fidelity interactions (Fig. 5A).

Our results support the hypothesis that the terminase in VZV is a tripartite complex formed by ORF25, ORF30 and ORF45/42 (Fig. 5A and B) similar as reported for HSV-1 [9] and PrV[2, 9] . As in HSV-1[26] (but not PrV[2]), ORF30 and ORF45/42 of the VZV terminase complex interacted with the portal protein ORF54 by Y2H and LuMPIS (Fig. 5A), In VZV, there was an additional interaction between the terminase complex and ORF54 via ORF25, which was detected by BRET and LuMPIS. We also detected novel interactions linking the packaging proteins ORF34, ORF43 and ORF26 to the terminase complex (ORF34-ORF25 and ORF43- ORF25). The interaction between ORF25 and ORF43 corresponds to the HSV-1 interaction UL33-UL17[11, 27] and represents a link between the capsid and the terminase complex as UL17 is located on the external surface of the viral capsid and thought to stabilize the capsid or engage molecular motors for capsid transport[28, 29]. The interaction between the tegument protein UL14 (ORF46) and UL33 (ORF25) described for HSV-1[17] was also detected in VZV by BRET (but neither Y2H nor LuMPIS). In VZV, we observed an interaction between the terminase complex and NEC mediated by ORF25 and ORF27 by all three types of binary interaction assays (Fig. 5A)[10,16]. In previous studies, multiple additional interactions (ORF45/42-ORF27; ORF34-ORF24; ORF26-ORF24; ORF25-ORF24) between terminase/associated proteins and NEC have been observed. The significance of the differences between VZV and other α-herpesviruses, however, remains

elusive, as direct conclusions can only be drawn if comparative studies were done using the same technologies and were done in parallel.

In summary, we present evidence that ORF25 is an essential protein and represents a central hub for the proteins involved in encapsidation and nuclear egress. In future work, it would be important to define its specific role as component of the terminase complex, for example as a scaffold and stabilizing component for other proteins involved in packaging and encapsidation.

## Supplementary Material

Refer to Web version on PubMed Central for supplementary material.

## Acknowledgments

Financial support by the Deutsche Forschungsgemeinschaft (BA 2035/3-1), the BMBF BioChancePLUS / FKZ: 0315182, the SPP1230 priority program “Mechanisms of gene vector entry and persistence”, the Friedrich-Baur-Stiftung, the Bavarian Genome Research Network (BayGene), NIH (grant AI053846) and LMUexcellent (grant 42595-6) is gratefully acknowledged.

## REFERENCES

1. Mettenleiter TC, Klupp BG, Granzow H. Herpesvirus assembly: an update. Virus Res. 2009; 143(2): 222–34. [PubMed: 19651457]
2. Fuchs W, Klupp BG, Granzow H, Leege T, Mettenleiter TC. Characterization of pseudorabies virus (PrV) cleavage-encapsidation proteins and functional complementation of PrV pUL32 by the homologous protein of herpes simplex virus type 1. J Virol. 2009; 83(8):3930–43. [PubMed: 19193798]
3. Higgs MR, Preston VG, Stow ND. The UL15 protein of herpes simplex virus type 1 is necessary for the localization of the UL28 and UL33 proteins to viral DNA replication centres. J Gen Virol. 2008; 89(Pt 7):1709–15. [PubMed: 18559942]
4. Beilstein F, Higgs MR, Stow ND. Mutational analysis of the herpes simplex virus type 1 DNA packaging protein UL33. J Virol. 2009; 83(17):8938–45. [PubMed: 19553324]
5. Koslowski KM, Shaver PR, Casey JT 2nd, Wilson T, Yamanaka G, Sheaffer AK, Tenney DJ, Pederson NE. Physical and functional interactions between the herpes simplex virus UL15 and UL28 DNA cleavage and packaging proteins. J Virol. 1999; 73(2):1704–7. [PubMed: 9882384]
6. Beard PM, Taus NS, Baines JD. DNA cleavage and packaging proteins encoded by genes U(L)28, U(L)15, and U(L)33 of herpes simplex virus type 1 form a complex in infected cells. J Virol. 2002; 76(10):4785–91. [PubMed: 11967295]
7. Addison C, Rixon FJ, Preston VG. Herpes simplex virus type 1 UL28 gene product is important for the formation of mature capsids. J Gen Virol. 1990; 71(Pt 10):2377–84. [PubMed: 2172450]
8. Baines JD, Cunningham C, Nalwanga D, Davison A. The U(L)15 gene of herpes simplex virus type 1 contains within its second exon a novel open reading frame that is translated in frame with the U(L)15 gene product. J Virol. 1997; 71(4):2666–73. [PubMed: 9060619]
9. Yang K, Homa F, Baines JD. Putative terminase subunits of herpes simplex virus 1 form a complex in the cytoplasm and interact with portal protein in the nucleus. J Virol. 2007; 81(12):6419–33. [PubMed: 17392365]
10. Uetz P, Dong YA, Zeretzke C, Atzler C, Baiker A, Berger B, Rajagopala SV, Roupelieva M, Rose D, Fossum E, Haas J. Herpesviral protein networks and their interaction with the human proteome. Science. 2006; 311(5758):239–42. [PubMed: 16339411]
11. Visalli RJ, Knepper J, Goshorn B, Vanover K, Burnside DM, Irven K, McGauley R, Visalli M. Characterization of the Varicella-zoster virus ORF25 gene product: pORF25 interacts with multiple DNA encapsidation proteins. Virus Res. 2009; 144(1-2):58–64. [PubMed: 19720242]
12. Vizoso Pinto MG, Villegas JM, Peter J, Haase R, Haas J, Lotz AS, Muntau AC, Baiker A. LuMPIS--a modified luminescence-based mammalian interactome mapping pull-down assay for

the investigation of protein-protein interactions encoded by GC-low ORFs. Proteomics. 2009; 9(23):5303–8. [PubMed: 19834906]

13. Vizoso Pinto MG, Pfrepper KI, Janke T, Noelting C, Sander M, Lueking A, Haas J, Nitschko H, Jaeger G, Baiker A. A systematic approach for the identification of novel, serologically reactive recombinant Varicella-Zoster Virus (VZV) antigens. Virol J. 2010; 7:165. [PubMed: 20646309]
14. Niizuma T, Zerboni L, Sommer MH, Ito H, Hinchliffe S, Arvin AM. Construction of varicella-zoster virus recombinants from parent Oka cosmids and demonstration that ORF65 protein is dispensable for infection of human skin and T cells in the SCID-hu mouse model. J Virol. 2003; 77(10):6062–5. [PubMed: 12719598]
15. Berarducci B, Rajamani J, Reichelt M, Sommer M, Zerboni L, Arvin AM. Deletion of the first cysteine-rich region of the varicella-zoster virus glycoprotein E ectodomain abolishes the gE and gI interaction and differentially affects cell-cell spread and viral entry. J Virol. 2009; 83(1):228–40. [PubMed: 18945783]
16. Stellberger T, Hauser R, Baiker A, Pothineni VR, Haas J, Uetz P. Improving the yeast two-hybrid system with permutated fusions proteins: the Varicella Zoster Virus interactome. Proteome Sci. 2010; 8:8. [PubMed: 20205919]
17. Yamauchi Y, Wada K, Goshima F, Takakuwa H, Daikoku T, Yamada M, Nishiyama Y. The UL14 protein of herpes simplex virus type 2 translocates the minor capsid protein VP26 and the DNA cleavage and packaging UL33 protein into the nucleus of coexpressing cells. J Gen Virol. 2001; 82(Pt 2):321–30. [PubMed: 11161269]
18. Cunningham C, Davison AJ. A cosmid-based system for constructing mutants of herpes simplex virus type 1. Virology. 1993; 197(1):116–24. [PubMed: 8212547]
19. Wang R, Brattain MG. The maximal size of protein to diffuse through the nuclear pore is larger than 60kDa. FEBS Lett. 2007; 581(17):3164–70. [PubMed: 17588566]
20. Reichelt M, Brady J, Arvin AM. The replication cycle of varicella-zoster virus: analysis of the kinetics of viral protein expression, genome synthesis, and virion assembly at the single-cell level. J Virol. 2009; 83(8):3904–18. [PubMed: 19193797]
21. Piehler J. New methodologies for measuring protein interactions in vivo and in vitro. Curr Opin Struct Biol. 2005; 15(1):4–14. [PubMed: 15718127]
22. Braun P, Tasan M, Dreze M, Barrios-Rodiles M, Lemmens I, Yu H, Sahalie JM, Murray RR, Roncari L, de Smet AS, Venkatesan K, Rual JF, Vandenhaute J, Cusick ME, Pawson T, Hill DE, Tavernier J, Wrana JL, Roth FP, Vidal M. An experimentally derived confidence score for binary protein-protein interactions. Nat Methods. 2009; 6(1):91–7. [PubMed: 19060903]
23. Mercier JF, Salahpour A, Angers S, Breit A, Bouvier M. Quantitative assessment of beta 1- and beta 2-adrenergic receptor homo- and heterodimerization by bioluminescence resonance energy transfer. J Biol Chem. 2002; 277(47):44925–31. [PubMed: 12244098]
24. Hamdan FF, Percherancier Y, Breton B, Bouvier M. Monitoring protein-protein interactions in living cells by bioluminescence resonance energy transfer (BRET). Curr Protoc Neurosci. 2006 Chapter 5, Unit 5 23.
25. Xu Y, Piston DW, Johnson CH. A bioluminescence resonance energy transfer (BRET) system: application to interacting circadian clock proteins. Proc Natl Acad Sci U S A. 1999; 96(1):151–6. [PubMed: 9874787]
26. White CA, Stow ND, Patel AH, Hughes M, Preston VG. Herpes simplex virus type 1 portal protein UL6 interacts with the putative terminase subunits UL15 and UL28. J Virol. 2003; 77(11):6351–8. [PubMed: 12743292]
27. Fossum E, Friedel CC, Rajagopala SV, Titz B, Baiker A, Schmidt T, Kraus T, Stellberger T, Rutenberg C, Suthram S, Bandyopadhyay S, Rose D, von Brunn A, Uhlmann M, Zeretzke C, Dong YA, Boulet H, Koegl M, Bailer SM, Koszinowski U, Ideker T, Uetz P, Zimmer R, Haas J. Evolutionarily conserved herpesviral protein interaction networks. PLoS Pathog. 2009; 5(9):e1000570. [PubMed: 19730696]
28. Kuhn J, Leege T, Granzow H, Fuchs W, Mettenleiter TC, Klupp BG. Analysis of pseudorabies and herpes simplex virus recombinants simultaneously lacking the pUL17 and pUL25 components of the C-capsid specific component. Virus Res. 2010

29. Wills E, Scholtes L, Baines JD. Herpes simplex virus 1 DNA packaging proteins encoded by UL6, UL15, UL17, UL28, and UL33 are located on the external surface of the viral capsid. J Virol. 2006; 80(21):10894–9. [PubMed: 16920825]

30. Schnee M, Ruzsics Z, Bubeck A, Koszinowski UH. Common and specific properties of herpesvirus UL34/UL31 protein family members revealed by protein complementation assay. J Virol. 2006; 80(23):11658–66. [PubMed: 17005637]

31. Lotzerich M, Ruzsics Z, Koszinowski UH. Functional domains of murine cytomegalovirus nuclear egress protein M53/p38. J Virol. 2006; 80(1):73–84. [PubMed: 16352532]

32. Jacobson JG, Yang K, Baines JD, Homa FL. Linker insertion mutations in the herpes simplex virus type 1 UL28 gene: effects on UL28 interaction with UL15 and UL33 and identification of a second-site mutation in the UL15 gene that suppresses a lethal UL28 mutation. J Virol. 2006; 80(24):12312–23. [PubMed: 17035316]

33. Yang K, Baines JD. The putative terminase subunit of herpes simplex virus 1 encoded by UL28 is necessary and sufficient to mediate interaction between pUL15 and pUL33. J Virol. 2006; 80(12): 5733–9. [PubMed: 16731912]

34. Visalli RJ, Nicolosi DM, Irven KL, Goshorn B, Khan T, Visalli MA. The Varicella-zoster virus DNA encapsidation genes: Identification and characterization of the putative terminase subunits. Virus Res. 2007; 129(2):200–11. [PubMed: 17868947]

35. Abbotts AP, Preston VG, Hughes M, Patel AH, Stow ND. Interaction of the herpes simplex virus type 1 packaging protein UL15 with full-length and deleted forms of the UL28 protein. J Gen Virol. 2000; 81(Pt 12):2999–3009. [PubMed: 11086131]

## Synopsis

Varicella zoster virus (VZV) ORF25 belongs to 40 core proteins conserved throughout the *Herpesviridae*. We investigated the interactions of all ten VZV proteins related to the encapsidation process and the nuclear egress complex (NEC) by three independent protein- protein interaction (PPI) assays: Y2H, LuMPIS and BRET. We demonstrate that ORF25 is essential for VZV replication, being a central hub linking encapsidation proteins and the NEC.

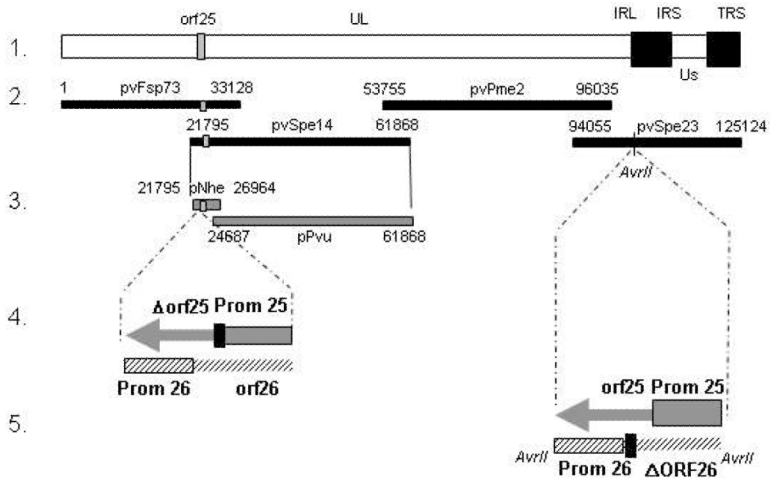


**Fig. 1.**

Construction of p-OKA cosmid vectors with VZV ORF25 deletion and substitution mutants. Line 1 shows a schematic diagram of the pOKA genome and the localization of orf25 in the unique long region. Line 2 depicts the overlapping segments of the pOKA genome subcloned into the respective pOKA cosmids: pvFspe73, pvSpe14, pvSpe23, and pvPme 2. Line 3 shows the splitting of the pvSpe14 segment into pNhe and pPvu. Line 4 shows the construction of the orf25 deletion mutant, where the second codon of orf25 was changed into a stop codon without affecting the integrity of the orf26 reading frame (black box). Line 5 depicts the position of the single *AvrII* site within pvSpe23 used for the insertion of orf25 rescue or substitution mutants. shows the construction of ORF25 mutants using a novel 5 cosmid system. Lane 1 shows the localization of ORF25 within the VZV genome and lane 2 the arrangement of the four cosmids including the whole VZV genome. Lane 3 shows how cosmid pvSpe14 was split into two overlapping cosmids. Lane 4 depicts the construction of the deletion mutant by introducing the stop codon TAA (black square) at aa position 2, which results in silent mutations for the overlapped ORF26. Lane 5 depicts the ectopic *AvrII* site of insertion of the rescue mutant.

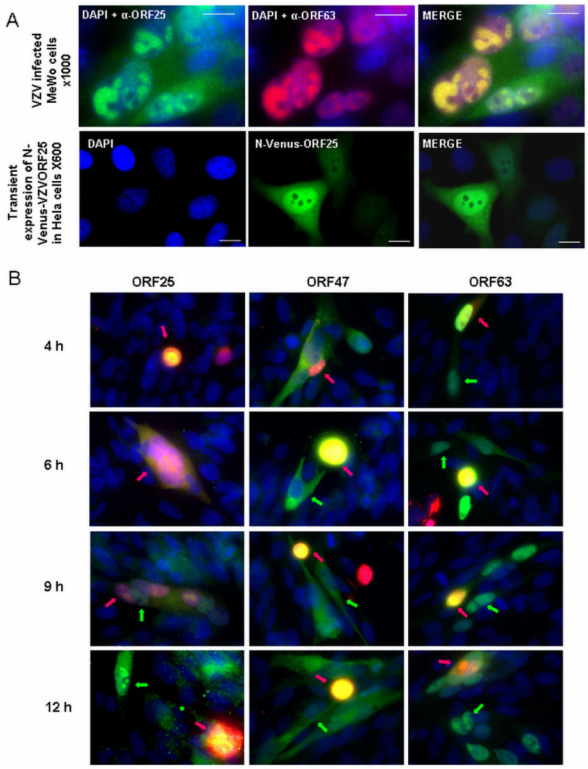


**Fig. 2.**

A) The upper panel shows MeWo cells that were infected with pOKA, fixed at 48 hpi and subjected to microscopic analysis. ORF25 was detected with a rabbit polyclonal anti-ORF25 and IE63 was detected with a mouse and nuclei were counterstained with DAPI. The lower panel shows MeWo cells transfected with the expression plasmid pCR3.1-N-Venus-ORF25 expressing full-length ORF25, fixed at 48 h post transfection, and subjected to microscopic analysis. B) Kinetics of ORF25 expression in VZV infected MeWo cells. The infected input cells were labeled with an orange cell tracker, which allows the selective analysis of newly infected cells. MeWo cells were infected with orange CellTracker labeled, pOKA-infected inoculum cells. The cells were fixed at 4, 6, 9 and 12 hpi and stained with specific antibodies for VZV proteins ORF25, ORF47 or ORF63. Cell nuclei were counterstained with DAPI. Pink arrows mark inoculum cells whereas green arrows indicate the corresponding VZV ORF.

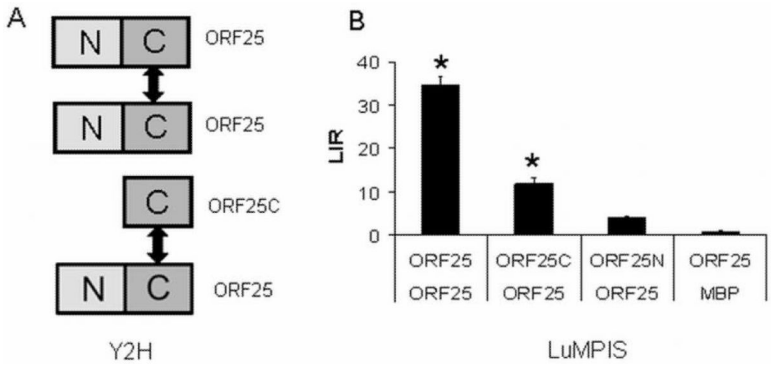


**Fig. 3.**

Self-interaction of ORF25. This figure shows the Y2H and LuMPIS results of the ORF25 self interaction assay as studied with the full-length protein as well as with its N- and C-terminal domains. The data were statistically analysed by ANOVA (*P<0.05) followed by Dunnett's post hoc test.

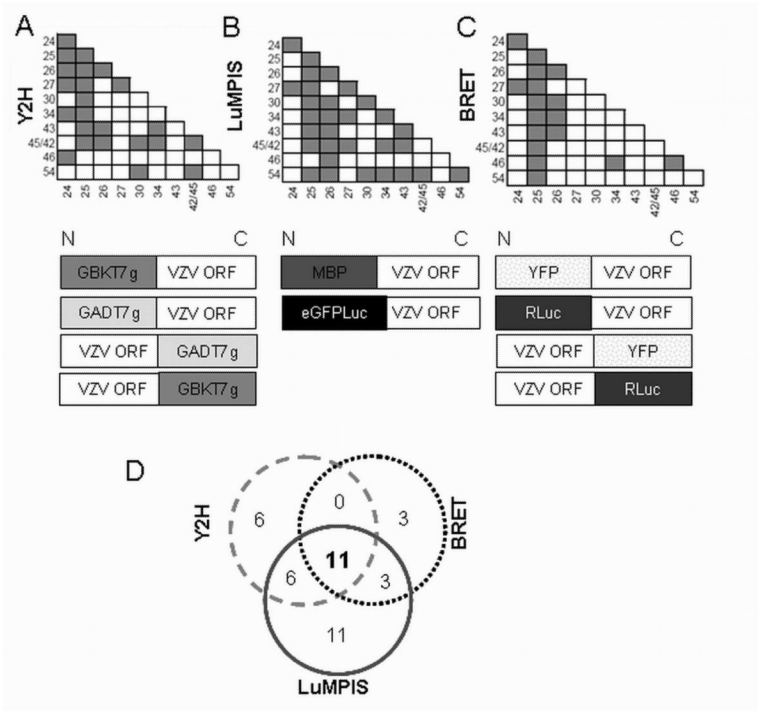


**Fig. 4.**

PPI of proteins putatively involved in encapsidation and nuclear egress as determined by three independent PPI screens. Panel A, B and C depict the results obtained by Y2H [10, 16], LuMPIS and BRET, a full box represents a positive interaction, under each matrix there is a scheme illustrating the different fusion proteins used in the respective assays. Panel D summarizes the number of in the intersections depict the overlap between the different screening systems.

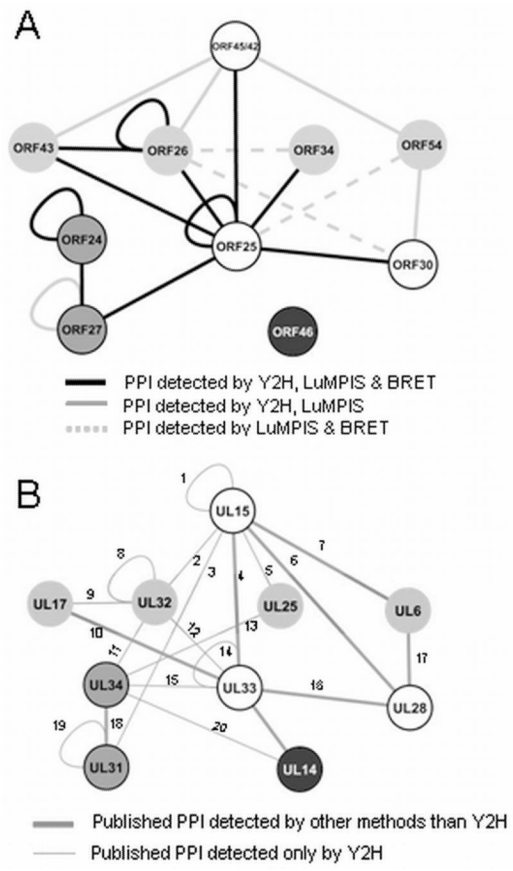


**Fig. 5.**

Model of the PPI network of proteins putatively involved in encapsidation and nuclear egress. Panel A shows the PPI considered as high fidelity (detected by all three screen systems) in black full lines, and those considered as medium fidelity (detected by two systems) in full grey line if detected by Y2H and LuMPIS and in dashed lines if detected by LuMPIS and BRET. Panel B depicts the interactions of the orthologues as already described in the literature [2, 3, 9-11, 16, 17, 26, 27, 30-33]. Full dark gray lines represent interactions validated with other systems than Y2H and the dashed lines represent PPI found exclusively in Y2H screens. The numbers on the lines represent respective citations **1**=[16, 34, 35], **2**=[16], **3**=[10], **4**=[3, 10, 16], **5**=[10], **6**= [2, 11, 32, 35], **7**=[26, 27], **8**=[10, 16], **9**=[16], **10**=[11, 16, 27], **11**=[16], **12**=[16], **13**=[10], **14**=[10, 16], **15**=[16], **16**=[2, 3, 10, 11, 33, 34], **17**=[26, 30, 31], **18**=[10, 16, 30, 31], **19**=[10], **20**=[16].

## Table 1

Summary of ORF25 PPIs with proteins related to the encapsidation and nuclear egress process as determined by three independent methods: Y2H, LuMPIS and BRET.

| PPI ORF25 vs. | Y2H | LuMPIS | BRET | Fidelity score |
|---|---|---|---|---|
| ORF24 | + | − | − | [a]l |
| ORF25 | + | + | + | [b]h |
| ORF26 | + | + | + | h |
| ORF27 | + | + | + | h |
| ORF30 | + | + | + | h |
| ORF34 | + | + | + | h |
| ORF43 | + | + | + | h |
| ORF45/42 | + | + | + | h |
| ORF46 | − | − | + | l |
| ORF54 | − | + | + | [c]m |

PPI detected were considered as [a]l: low confident if detected by only one method, [b]h: highly confident if detected by all three systems and as [c]m: medium confident if detected by two methods.